Article:
Marino, S., Hannemann, N., Bishop, R.T. et al. (12 more authors) (2022) Anti-inflammatory, but not osteoprotective, effect of the TRAF6/CD40 inhibitor 6877002 in rodent models of local and systemic osteolysis. Biochemical Pharmacology, 195. 114869. ISSN 0006-2952

https://doi.org/10.1016/j.bcp.2021.114869

Anti-inflammatory, but not osteoprotective, effect of the TRAF6/CD40 inhibitor 6877002 in rodent models of local and systemic osteolysis

AUTHORS/AFFILIATIONS

Silvia Marino[1,2*], Nicole Hannemann[3]*, Ryan T. Bishop[1], Feier Zeng[1], Giovana Carrasco[1], Sandrine Meurisse[4], Boya Li[1], Antonia Sophocleous[5], Anna Sparatore[6], Tobias Baeuerle[7], Slobodan Vukicevic[8], Marielle Auberval[4], Patrick Mollat[4], Aline Bozec[3] and Aymen I. Idris[1,2]

*Authors contributed equally to manuscript.

[1]Department of Oncology and Metabolism, University of Sheffield, Medical School, Beech Hill Road, Sheffield, S10 2RX, UK.

[2]Bone and Cancer Group, Edinburgh Cancer Research Centre, MRC Institute of Genetics and Molecular Medicine, University of Edinburgh, EH4 2XR, UK.

[3]Department of Internal Medicine, 3-Rheumatology and Immunology, Friedrich-Alexander University Erlangen-Nürnberg (FAU) and Universitätsklinikum Erlangen, Erlangen, German.

[4]Galapagos SASU, 102 Avenue Gaston Roussel, 93230 Romainville, France.

[5]Department of Life Sciences, School of Sciences, European University Cyprus, 6 Diogenes Street, 1516, Nicosia, Cyprus.

[6]University of Milano, Department of Pharmaceutical Science, Milan, Italy.

[7]Institute of Radiology, Friedrich-Alexander-Universität Erlangen-Nürnberg and Universitätsklinikum, Erlangen, Bayern, Germany.

[8]Department of Anatomy, Medical School, University of Zagreb, Zagreb, Croatia.

RUNNING TITLE

TRAF6 inhibition reduces arthritis progression

CORRESPONDENCE TO

Dr Aymen I. Idris. Department of Oncology and Metabolism, Medical School, Beech Hill Road, Sheffield, S10 2RX, UK. E-mail: aymen.idris@sheffield.ac.uk.

KEYWORDS

NFκB; TNFα; T-cell; osteoclast; ovariectomy; inflammation.

ABBREVIATIONS

Alk Phos, alkaline phosphatase; ALN Alendronate; ALZ, alizarin red; ANOVA, analysis of variance; BM, bone marrow; BSA, bovine serum albumin; BV, bone volume; CD40, Cluster of differentiation 40; DMSO, Dimethyl sulfoxide; ERK, extracellular signal-regulated protein kinase; FCS, fetal calf serum; IKK, IκB kinase; IL, Interleukin; IRAK, IL1β receptor adaptor protein; JNK, c-Jun N-terminal kinase; L, ligand; MAP, mitogen-activated protein; M-CSF, macrophage colony-stimulating factor; MEM, minimum essential medium; microCT, micro–computed tomography; mm, millimeter; MRI, magnetic resonance imaging; NFκB, nuclear factor kappa-light-chain-enhancer of activated B cells; OPG, osteoprotegerin; ovx, ovariectomy; PBMC, peripheral blood mononuclear cell; PBS, phosphate buffered saline; RA, Rheumatoid arthritis; RANK, receptor activator of NFκB; RANKL, RANK ligand; SD, standard deviation; TNFα, tumour necrosis factor alpha; TRAcP, tartrate-resistant acid phosphatase; TRAF, tumour necrosis factor receptor-associated factor.

ABSTRACT

NFκB plays a key role in inflammation and skeletal disorders. Previously, we reported that pharmacological inhibition of NFκB at the level of TRAF6 suppressed RANKL, CD40L and IL1β-induced osteoclastogenesis and attenuated cancer-induced bone disease. TNFα is also known to regulate TRAF6/NFκB signalling, however the anti-inflammatory and osteoprotective effects associated with inhibition of the TNFα/TRAF6/NFκB axis have not been investigated. Here, we show that *in vitro* and *ex vivo* exposure to the verified small-molecule inhibitor of TRAF6, 6877002 prevented TNFα-induced NFκB activation, osteoclastogenesis and calvarial osteolysis, but it had no effects on TNFα-induced apoptosis or growth inhibition in osteoblasts. Additionally, 6877002 disrupted T-cells support for osteoclast formation and synoviocyte motility, without affecting the viability of osteoblasts in the presence of T-cells derived factors. Using the collagen-induced arthritis model, we show that oral and intraperitoneal administration of 6877002 in mice reduced joint inflammation and arthritis score. Unexpectedly, no difference in trabecular and cortical bone parameters were detected between vehicle and 6877002 treated mice, indicating lack of osteoprotection by 6877002 in the arthritis model described. Using two independent rodent models of osteolysis, we confirmed that 6877002 had no effect on trabecular and cortical bone loss in both osteoporotic rats or RANKL- treated mice. In contrast, the classic anti-osteolytic alendronate offered complete osteoprotection in RANKL- treated mice. In conclusion, TRAF6 inhibitors may be of value in the management of the inflammatory component of bone disorders, but may not offer protection against local or systemic bone loss, unless combined with anti-resorptive therapy such as bisphosphonates.

GRAPHICAL ABSTRACT

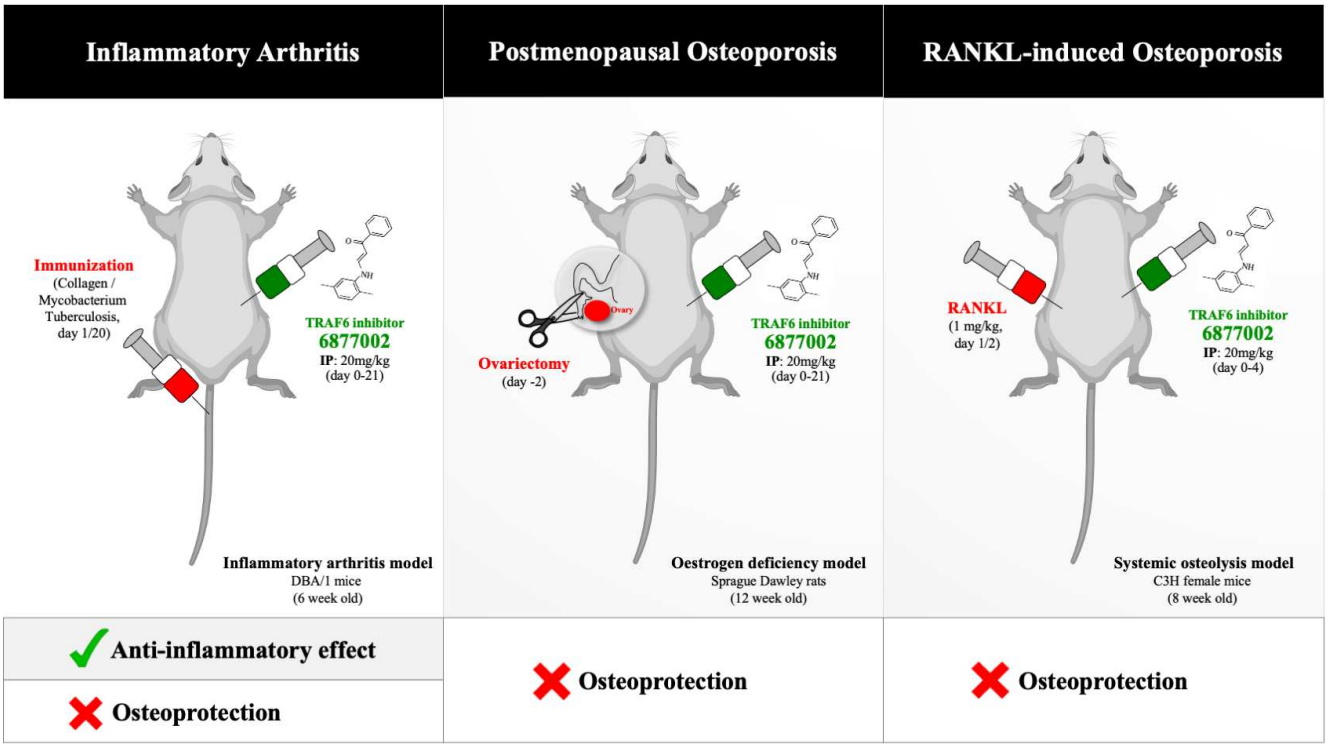

HIGHLIGHTS

- The verified TRAF6/NF□B inhibitor 6877002 inhibited TNF□-induced osteoclastogenesis *in vitro*, inflammatory osteolysis *ex vivo* and arthritis progression *in vivo*.
- 6877002 failed to affect systemic bone loss in rodents models of arthritis, osteopetrosis or RANKL-induced osteolysis.
- TRAF6 inhibitors can be of value in the management of inflammatory bone disorders.
- However, these agents may not offer osteoprotection comparable to anti-resorptive agents in clinical practice.

1. INTRODUCTION

Inflammation is a major contributor to bone destruction, disability and co-morbidities associated with skeletal disorders, particularly rheumatoid arthritis (RA), and to a lesser degree postmenopausal osteoporosis [1, 2]. A number of treatments that antagonise the action of proinflammatory mediators have been developed [3]. However, many of these strategies were deemed less effective due to drug failure at preclinical testing, lack of clinical efficacy, rise in acquired drug resistance and/or development of adverse effects [3-5]. Tumour necrosis factor (TNF) receptor-associated factor 6 (TRAF6) is an adaptor protein for various receptors for proinflammatory and osteolytic factors that share a distinctive TRAF6/CD40-binding motif [6-9]. The list includes receptor activator of NFκB (RANK), Cluster of differentiation 40 (CD40) and interleukin-1β (IL-1β) receptor-associated kinase (IRAK). Recruitment of TRAF6 by receptors for these ligands activates a number of intracellular signalling pathways including the IκB kinase (IKK)/NFκB signal transduction and mitogen-activated protein (MAP) kinase pathways [8, 10-15]. In the skeleton, genetic and pharmacological studies have confirmed that TRAF6-mediated IKK/NFκB activation is a prerequisite for RANKL-induced osteoclastogenesis [8, 14-19], and it also plays an essential role in the regulation of bone loss associated with excessive activity of CD40L, IL1β and transforming growth factor - β (TGFβ) [14-19]. Collectively, findings to date consolidated the critical role of TRAF6 in the regulation of joint and bone diseases, particularly RA and osteoporosis.

TNFα is the master regulator of inflammation-related joint and bone destruction, and TNF inhibitors are clinically effective anti-rheumatic agents [20-22]. Emerging evidence suggests that TNFα utilizes both TRAF6 and TRAF2 to influence NFκB signalling [23-25], however the role of the TNFα/TRAF6 axis in the development and progression of

inflammatory bone and joint diseases remains poorly understood. We have previously reported that a verified small-molecule inhibitor of TRAF6/CD40 signalling, called 6877002 [26], inhibited RANKL, CD40 and IL1β–induced osteoclastogenesis *in vitro* and cancer-induced bone disease in mice [27]. Bearing in mind that TNFα is known to cooperate together with CD40L, RANK and IL1β to regulate TRAF6/NFκB signalling [20, 22] and bone and joint destruction [23-25, 28], we carried out extensive *in vitro*, *ex vivo* and *in vivo* investigations to examine the efficacy of 6877002 as anti-inflammatory and/or osteo-protective agent. These studies showed that exposure to 6877002 was accompanied by significant reduction in TNFα–induced osteoclast formation *in vitro* and inflammatory calvarial osteolysis *ex vivo*. *In vivo*, oral and intraperitoneal administration of 6877002 reduced collagen-induced joint inflammation and arthritis score. Unexpectedly, the administration of 6877002 failed to offer osteoprotective effect against arthritis, ovariectomy or RANKL-associated systemic bone loss. Thus, inhibitors of TRAF6/CD40 signalling such as 6877002 may be of value in the treatment of arthritis, but must be part of a treatment regime that includes an anti-resorptive therapy to ensure protection against systemic bone loss.

2. MATERIALS AND METHODS

2.1 Reagents and cell lines

The small-molecule inhibitor of TRAF6 6877002 (3-[(2,5-Dimethylphenyl)amino]-1-phenyl-2-propen-1-one, Fig. 1, panel a) was a kind gift from G. Nicolaes (Maastricht University, Maastricht, The Netherlands) and E. Lutgens (University of Amsterdam, The Netherlands), and this agent was also purchased from Tocris Biosciences (Abingdon, UK). Mouse RAW 264.7 and MC3T3-E1 and human SW982, Saos2 and T Jurkat E6.1 cell-lines were purchased from the American type culture collection (ATCC, Manassas, Virginia, USA). Mouse macrophage

colony stimulating factor (M-CSF) was purchased from R&D Systems (Abingdon, UK), human IL1β from Roche (London, UK), TNFα from R&D Systems (Abingdon, UK) and soluble RANKL (sRANKL) from Galapagos SASU (Romainville, France). Chicken collagen type II and incomplete Freund's adjuvant were purchased from Sigma-Aldrich (Taufkirchen, Germany), and Mycobacterium tuberculosis from Difco Laboratories (Detroit, United States). The minimum essential mediums (MEM) alpha(a)-MEM, delta(D)-MEM, dimethyl sulfoxide (DMSO), Tween 20, Saline, bovine serum albumin (BSA) and phosphate buffered saline (PBS) were obtained from ThermoFisher (Leicestershire, UK), and RPMI medium was purchased from Sigma-Aldrich (Dorset, UK).

2.2 Mice experiments

All *in vivo* animal experimentations and protocols were approved by local Ethics Committees. The safety profile of the TRAF6 inhibitor 6877002 was previously reported in pharmacological studies that showed daily treatment with this agent exerts no negative effects on hematopoiesis with up to 6 weeks of treatment mice [27, 29]. In the present study, we observed no overt signs of toxicity nor significant change in body weight (data not shown).

2.2.1 Mouse model of joint inflammatory arthritis

Arthritis-associated joint inflammation and systemic bone loss were studied using the mouse collagen-induced arthritis (CIA) model [30]. Briefly, male DBA/1 mice (6 week-old, Freiburg, Germany) were anesthetized and received intradermal (ID) injection of an emulsion of chicken collagen type II (100µl, 2 mg/mL) in complete Freund's adjuvant supplemented with freeze-dried Mycobacterium tuberculosis (1 mg/mL) at the base of the tail [30]. Inflammation of the paws was first observed after approximately 2 weeks. At this stage, mice were randomly allocated into 4 groups (8 mice/group), and were subjected to intraperitoneal (IP, 20 mg/kg/thrice-weekly) or oral (gavage, 50 mg/kg/thrice-weekly) administration of

6877002. Controls received vehicle (DMSO/Tween20/Saline, 1:1:8) alone. Treatments were continued for 21 days, mice were scored for arthritis severity on day 23 and every 48 hours till mice were sacrificed on day 45 [30]. Systemic bone loss was assessed at the tibia by micro-computed tomography (microCT, Bruker, Belgium) [30, 31]. For magnetic resonance imaging (MRI, Bruker, Belgium), excised hind legs were embedded and standard T1 and T2-weighted gradient echo sequence was used for segmentation of the soft tissue.

2.2.2 Rat model of oestrogen deficiency associated osteolysis

The rat oestrogen deficiency model was used to test the anti-resorptive effect of 6877002. Female Sprague Dawley rats (4-5 month-old, Harlan Laboratories, Croatia) were subjected to ovariectomy or sham operation (n = 9/group) [32], and 6877002 was administered by IP injection (20 mg/kg/thrice-weekly) two days post ovariectomy or sham operation. Controls received vehicle (DMSO/Tween20/Saline, 1:1:8) alone. Treatment was continued for 3 weeks, and skeletal properties were evaluated at the tibia by microCT (resolution, 19 μm) [31].

2.2.3 Mouse model of RANKL-induced osteolysis.

The mouse RANKL model was used to examine the anti-resorptive effect of 6877002 on TRAF6-driven systemic bone loss. Female C3H mice (8 week-old, Janvier labs, Le Genest-Saint-Isle, France) received IP injection of either 6877002 (10 and 20 mg/kg, 10 mice/group) for 4 consecutive days or Alendronate (ALN, 40 μg/kg, Key Organics, Camelford, UK) on day -3, 0 and 2. Sham and sRANKL control groups (10 mice/group) received vehicle (DMSO/Tween20/Saline, 1:1:8). On Day 1 and 2, sham control received vehicle (DMSO/PBS, 1:20) alone and the remaining 4 groups received IP injections of sRANKL (1 mg/kg, batch number GG347-019P). Mice were sacrificed on day 5, and skeletal properties were assessed at the tibia by microCT (resolution, 9 μm) [31].

2.2.4 Mouse calvarial model of inflammatory osteolysis.

The effects of 6877002 on TNFα-induced bone loss was studied *ex vivo* using the mouse calvarial organ culture [33]. Briefly, mouse calvarias were isolated from 2-day-old CD1 mouse neonates (Harlan Laboratories, UK), each half of the calvarial bone was cultured on stainless steel rafts in standard α-MEM tissue culture medium supplemented with either TNFα (20 ng/ml) or vehicle (1% BSA) in the presence and absence of 6877002. Cultures were terminated after 7 days and osteolysis was assessed by microCT (resolution, 5 μm) [31].

2.3 Osteoclast cultures and assays

The effects of 6877002 on TNFα-induced osteoclast formation was studied in mouse BM and RAW 264.7 cells, and human peripheral blood mononuclear cells (PBMCs). Mouse pre-osteoclasts were generated from BM cells flushed from the long bones of 3-5 month-old mice (Harlan Laboratories, UK), and cultured in standard α-MEM supplemented with M-CSF (200 ng/ml) for 48 hours [34]. M-CSF-dependent osteoclast precursor cells were plated into tissue culture plates in standard α-MEM supplemented with M-CSF (25 ng/ml) and RANKL (50 or 100 ng/ml) for 24 hours, prior the addition of TNFα (20 ng/ml). Mouse osteoclasts were also generated in cultures of mouse RAW 264.7 pre-osteoclast-like macrophages cultured in the presence of RANKL (100 ng/ml). Human osteoclasts were generated from PBMCs collected from healthy donors in accordance with the study protocol approved by the University of Sheffield Research Ethics Committee. CD14+ monocytes were isolated from the buffy coat using anti-CD14 antibody bound beads (Miltenyi Biotech, Gladbach, Germany), plated in standard α-MEM supplemented with M-CSF (25 ng/ml) and RANKL (30 ng/ml). Mature osteoclasts were identified using Tartrate-Resistant Acid Phosphatase (TRAcP) staining as previously described in [34].

2.4 Osteoblast cultures and assays

Osteoblasts were isolated from the calvarial bone of 2-day-old mice or generated from mouse MC3T3-E1 and human Saos2 pre-osteoblast cells [35]. For osteoblast – osteoclast co-cultures, osteoblasts were cultured with BM cells flushed from the long bones of 3-5 month-old mice in standard α-MEM supplemented with 1,25-(OH)2-vitamin D3 (10 nM, Sigma-Aldrich, Dorset, UK) for 48 hours, prior exposure to TNFα (20 ng/ml) in the presence or absence of 6877002 (10 μM) for 72 hours. For bone nodule formation assay, osteoblasts were incubated for up to 21 days in standard α-MEM supplemented with β-glycerol phosphate (10 μM, ThermoFisher, Leicestershire, UK) and L-ascorbic acid (50 μg/ml, Sigma-Aldrich, Dorset, UK). Osteoblast growth and bone nodule formation were determined by AlamarBlue (Invitrogen, Paisley, UK) and alizarin red (ALZ, Sigma-Aldrich, Dorset, UK) staining, respectively [35, 36]. Osteoblast apoptosis was detected using Apo-ONE® Homogeneous Caspase-3/7 Assay (Promega, Southampton, UK).

2.5 T-Cells and conditioned medium

The human T-cell-like Jurkat E6.1 cell lines were cultured in standard RPMI tissue culture medium. For studies involving T-cell conditioned medium, Jurkat E6.1 cells were incubated in serum free RPMI medium for 16 hours, conditioned medium was removed, filtered (0.22 μm filter diameter) and added to cultures of osteoclasts, osteoblasts and SW982 synoviocyte cultures at 20% (v/v), for the desired period [33].

2.6 Mechanistic studies

Western blot analysis was used to study the expression of TRAF6, and effects of 6877002 on NFκB and MAPK activation [37]. Briefly, cultures were incubated in serum free medium for 60 minutes, and 6877002 or vehicle (0.1% DMSO) was added for the desired period of time in the presence and absence of tested cytokine. Cultures were homogenized in standard lysis buffer and protein (50 - 70 μg) was resolved by SDS-PAGE (BioRAD, Exeter, UK) and

immunoblotted with antibodies. Detection of native and phosphorylated proteins was performed using the anti-TRAF6, anti-phospho IκBα Ser36 and anti-IκB, phospho-p42/44, total p42/44, phospho-P38, total P38, phospho-JNK1/2 and total JNK (1:1000 dilution, Cell Signalling Technology, London, UK). Immuno-complexes were detected using horseradish peroxidase-conjugated secondary antibody (1:1000 dilution, Stratech Scientific Unit, Suffolk, UK). The rabbit anti-actin (Sigma-Aldrich, Dorset, UK) was used as standard. Membranes were visualised using chemiluminescence (Amersham, UK) on a ChemiDocMP imaging system (Biorad, Exeter, UK).

2.7 Statistical analysis

Results were reported as mean ± standard deviation (SD) unless otherwise stated. Comparison between three groups was done by analysis of variance (ANOVA) and student T-test was utilized to perform statistical between two groups (GraphPad Prism, La Jolla California, USA). A p-value of 0.05 or below was considered statistically significant.

3. RESULTS

3.1 6877002 inhibits TNFα-induced osteoclastogenesis and osteolysis

TNFα is implicated in the regulation of TRAF6 signalling [23-25, 28], and numerous studies have shown that TNFα enhances RANKL-induced osteoclastogenesis [20, 38]. Thus, we first utilized the mouse calvarial organ culture system (Fig. 1b) to examine the anti-TNFα and osteoprotective effects of the verified TRAF6 inhibitor 6877002 *ex vivo*. As shown in Figure 1 (panels b and c), TNFα caused significant loss of bone volume in mouse calvarial bone, and pre-treatment with 6877002 (10 μM) for 1 day prior the addition of TNFα (20 ng/ml) for 5 days completely reversed this effect (Fig.1c). Additionally, 6877002 (10 μM) enhanced bone volume in the absence of TNFα, suggesting an osteoprotective effect (Fig. 1c). Next, we

show that pre-treatment of osteoclast precursors with 6877002 for 1 hour after exposure to RANKL (50 and 100 ng/ml), but prior the addition of TNFα (20 ng/ml), reduced osteoclast formation in a concentration dependent manner (Fig. 1d-e). Of note, 6877002 (0-3 μM) had no effect on the proliferation of osteoclast precursors (Fig. 1f), excluding the possibility that the anti-osteoclast effect observed in TNFα and RANKL stimulated cultures (Fig. 1d) was mediated by a cytotoxic effect. Further mechanistic studies in mouse RAW 264.7 pre-osteoclasts showed that 6877002 prevented TNFα-induced canonical NFκB activation, as evidenced by significant inhibition in IκBα phosphorylation (Fig. 1g, left), coupled with a modest, non-significant increase in total IκB (Fig. 1g, right). Representative photomicrographs from western blots from these experiments are shown in Fig. 1h.

3.2 6877002 has no effect on TNFα-related osteoblast inhibition

TNFα is known to enhance osteoblast support for osteoclastogenesis and to induce osteoblast apoptosis [20]. Thus, we examined the effects of 6877002 on *in vitro* osteoblast viability, apoptosis, bone nodule formation and support for osteoclastogenesis in the presence and absence of TNFα. First, we confirmed that pre-treatment of calvarial osteoblasts with 6877002 (10 μM) for 1 hour before exposure to TNFα (20 ng/ml), significantly reduced the number of multi-nucleated TRAcP positive osteoclasts in osteoblast – BM cell co-cultures after 72 hours (Fig. 1i). Next, we went on to show that prolonged exposure to TNFα reduced the *in vitro* cell viability (Fig. 1j) and induced caspase-3/7 activation (Fig. 1k) in osteoblasts after 5 days of continuous exposure, whereas pre-treatment with 6877002 neither prevented nor exacerbated these effects. Similarly, exposure to non-cytotoxic concentrations of 6877002 for 21 days (0 – 0.3 μM, Fig. 1l, left) had no effect on the ability of calvarial osteoblasts to form bone nodules *in vitro* (Fig. 1l, right).

3.3 6877002 disrupts T-cell crosstalk with synoviocytes and osteoclasts, but not with osteoblasts

TRAF6/CD40 is implicated in the regulation of the crosstalk between T lymphocytes and synovial and bone cells [39, 40]. With this in mind, we tested the effects of 6877002 on the ability of T-cells to grow and to influence synoviocyte motility, osteoclast formation and osteoblast proliferation *in vitro*. First, we demonstrated that conditioned medium from activated T-cells enhanced the 2D migration of the synoviocyte SW982 cells after 16 hours, and 6877002 pre-treatment (3 μM) significantly reduced this effect (Fig. 2a). Of importance, this effect was observed at a concentration (3 μM) that had no effect on the proliferation of SW982 cells (IC_{50} = >100 μM after 24 and 48 hours, and 49.28 ± 8.16 μM after 72 hours) or T-cells (IC_{50} = >100 μM after 24 and 48 hours, and 18.64 ± 6.93 μM after 72 hours). This excludes the possibility that the anti-migratory effect of this agent was due to reduction in synoviocyte viability. 6877002 (3 μM) reduced osteoclast number when cultured in RANKL (100 ng/ml) and conditioned medium from T-cells (20% v/v, Fig. 2b), without affecting pre-osteoclast survival (Fig. 2c). Furthermore, we examined the effects of 6877002 on T-cell – osteoblast interaction and observed that neither this agent nor conditioned medium from T-cells had any effect on osteoblast growth in the model described (Fig. 2d).

3.4 Oral and intraperitoneal treatments with 6877002 reduced inflammatory arthritis in mice

Guided by the aforementioned *in vitro* and *ex vivo* findings as well as our published work [27], we validated the anti-inflammatory effect of 6877002 in the mouse CIA model [30]. Figure 3 shows graphic representation and experiment timeline of intraperitoneal (IP, Fig. 3a) and oral (Fig. 3b) administration of 6877002 in 6 week-old DBA/1 mice (n = 10/group) for 23 days post the development of CIA. First, we observed that IP treatment with 6877002 (20 mg/kg/thrice/weekly) reduced the development of the inflammatory component of CIA, as

evident from the significant reduction in both paw thickness (Fig. 3c and d) and joint score (Fig. 3e). These effects were observed post the development of the disease on day 35 and were maintained to the end of the experiment on day 44 (Fig. 3). Encouraged by these results, we went on to perform an additional mouse experiment (Fig. 3b) that revealed that oral administration of 6877002 (50 mg/kg) was relatively less efficacious in halting the disease progression, but treated mice still exhibited significant reduction in paw thickness, evidenced by the significant reduction in area under the curve (AUC, Fig. 3c). Next, we carried out detailed MRI analysis to examine signs of hypervascularization and oedema in inflamed paws. As shown in Figure 3 (panels f and g), IP administration of 6877002 exerted significant reduction in T1 relaxation time in soft tissue (Fig. 3f, left), whereas mice that received oral treatment exhibited similar reduction in T2 relaxation time (Fig. 3f, right), indicative of reduced tissue water content. In the bone marrow, oral treatment with 6877002 was accompanied by significant reduction in T2 relaxation time (Fig. 3g), indicative of reduced bone marrow adiposity, whereas IP treatment had no significant effect. Representative photomicrographs of MRI images of the mouse hind paws from the experiment described are shown in Fig. 3, panels h and i. Notably, neither IP treatment nor oral administration of 6877002 led to significant changes in mouse body weight in the experiment described (data not shown). These findings together show that 6877002 treatment reduces the inflammatory component of arthritis in the mouse model described.

3.5 6877002 has no effect on systemic bone loss in arthritic mice and osteoporotic rats

RA is also characterised by systemic bone loss [1-3]. Thus, we next carried out detailed microCT analysis at the tibia of arthritic mice (Fig. 3) to look for signs of osteoprotection by 6877002. As shown in Figure 4, we detected no differences in trabecular bone volume/total

volume (Tb.BV/TV; Fig. 4a), number (Tb.N; Fig. 4b), thickness (Tb.Th; Fig. 4c) or separation (Tb.Sp; Fig. 4d) between vehicle or IP or oral 6877002 treated groups. Representative photomicrographs of microCT analysis of the trabecular compartment at the tibia from the experiment described are shown in Fig. 4e. Similarly, no differences in cortical bone volume (Ct.BV/TV, Fig. 4f) or thickness (Tb.Th; Fig. 4g) were detected between the vehicle and two 6877002 treated groups. Representative photomicrographs of microCT analysis of the cortical compartment at the tibia from the experiment described are shown in Fig. 4h.

Previous studies have shown that TRAF6/CD40 signalling regulates bone loss associated with oestrogen deficiency in osteoporotic rodents [40, 41]. Thus, we took the decision to investigate the effect of 6877002 on systemic bone loss in female Sprague Dawley rats (4-5 month-old) subjected to ovariectomy for 3 weeks (Fig. 5a). As expected, oestrogen deficiency (Fig. 5a) resulted in significant reduction in trabecular bone volume/total volume (BV/TV) in the tibia (Fig. 5b, left) and femur (Fig. 5b, middle) of these osteoporotic rats, and these effects were unaffected by IP administration of 6877002 (20 mg/kg). This agent also failed to affect trabecular BV/TV in the spine (Fig. 5b, right) or cortical BV/TV (Fig. 5c) in the tibia and femur. Representative photomicrographs of microCT analysis of rat trabecular and cortical compartments at the tibia, femur and spine from the experiment described are shown in Fig. 5 panels d, e and f, respectively.

3.6 6877002 has no significant effects on RANKL-induced MAP kinase activation

During the course of this investigation, we became aware of previous studies that showed TRAF6 interacts differently with multiple receptor associated factors and adaptor proteins to regulate signal transduction pathways, in particular NFκB and MAP kinase [10, 11, 42]. As both CD40 and RANK receptors share the same binding motif for TRAF6 targeted by

6877002, we carried out mechanistic studies that examined the effects of this agent on RANKL-induced NFκB and MAP kinase activation in mouse M-CSF dependent osteoclast precursors. As shown in Figure 6a, pre-exposure of preosteoclasts to 6877002 (10 – 30 μM) for 1 hour completely abolished RANKL (200 ng/ml) - induced IκBα phosphorylation in pre-osteoclasts, indicative of inhibition of canonical NFκB signalling. In these cultures, RANKL (200 ng/ml) also stimulated the phosphorylation of extracellular signal-regulated protein kinase 42 (ERK42) and to a lesser level ERK44, and these effects were unaffected by 6877002 (10 – 30 μM) (Fig. 6a, middle panels). Interestingly, RANKL (200 ng/ml) failed to stimulate the phosphorylation of P38 and c-Jun N-terminal kinases 1/2 (JNK1/2) in these cultures, whereas exposure to 6877002 at 30 μM was stimulatory (Fig. 6a, right panels). These mechanistic studies imply that 6877002 treatment is insufficient to inhibit RANKL-induced ERK1/2 MAP kinase activation in osteoclast precursors at concentrations that completely abolished canonical NFκB activation.

3.7 6877002 has no significant effects on RANKL-induced bone loss in mice

In view of the aforementioned mechanistic studies, we carried out an additional *in vivo* experiment to test whether administration of 6877002 affects RANKL/TRAF6-driven bone loss in mice. Figure 6 (panels b and c) show graphic representation (Fig. 6b) and experiment timeline (Fig. 6c) of intraperitoneal administration of 6877002 in 8 week-old C3H female mice (n = 10 mice/group). The classic anti-osteoclast bisphosphonate ALN was included as a positive control [43]. Detailed microCT analysis of the tibia from mice injected with sRANKL (1 mg/kg) showed that pre-treatment of mice with 6877002 (20 mg/kg) caused a non-significant trend towards reduction in trabecular bone loss (Tb.BV/TV; Fig. 6d). Representative photomicrographs of microCT images of the trabecular compartment at the tibia from the

experiment described are shown in Fig. 6e. Further analysis of bone architecture at the trabecular compartment demonstrated that 6877002 (10 and 20 mg/kg) had no significant effect on RANKL-induced loss in trabecular number (Tb.N; Fig. 6f), thickness (Tb.Th; Fig. 6g) or separation (Tb.Sp; Fig. 6h). In contrast, subcutaneous injection of ALN (60 μg/kg) completely abolished these effects (Fig. 6d-g). Of note, administration of sRANKL (1 mg/kg) had no effect on mouse body weight in the experiment described (data not shown).

4. DISCUSSION

In this study, we used the verified small-molecule inhibitor of TRAF6/CD40 6877002 to test the hypothesis that inhibition of TNFα-induced NFκB activation at the level of TRAF6 alleviates inflammatory and osteolytic components of joint and bone diseases in rodents. Our findings partially support this hypothesis. To explore the anti-inflammatory and osteoprotective properties of 6877002, we utilized standard *in vitro* and *ex vivo* models to show that 6877002 inhibited canonical NFκB activation by TNFα and this was accompanied by reduction in RANKL- and osteoblast-induced osteoclast formation and inflammatory calvarial osteolysis. However, it is important to note that these effects were observed in RANKL-stimulated cultures, and the *ex vivo* organ culture model that relies on the presence and action of RANKL, and a plethora of factors that directly (IL1β, CD40L and RANKL) or indirectly (TGFβ and IGF-1) activate TRAF6. We have previously showed that 6877002 completely abolished IL1β, CD40L and RANKL-induced NFκB activation and osteoclast formation [27], but it remains to be seen if 6877002 affects the actions of other bone-derived factors such as TGFβ. Nevertheless, osteoblasts and T-cells secrete IL1β, CD40L, RANKL and TNFα, and our present data indicate that 6877002 disrupted the ability of these cells to support osteoclastogenesis. In a similar vein, 6877002 inhibited T-cells support for synoviocyte

motility. Thus, it is reasonable to conclude that the anti-TNFα and anti-osteolytic effects of 6877002 were mediated – at least in part – by its ability to antagonize the action of TRAF6-activating inflammatory factors in the models described.

The *in vivo* data from the mouse CIA model partially complement this conclusion, and showed that 6877002 reduced joint inflammation and slowed down the disease progression, consistent with TNFα inhibition [20, 22]. An unexpected finding from this experiment is that IP injection of 6877002 at a dose of 20 mg/kg was more effective in reducing paw thickness and disease progression than a higher oral dose of 50 mg/kg. We also observed that IP and oral treatments caused inconsistent reduction in signs of hypervascularization and oedema in inflamed mouse paws. Whilst we cannot readily explain these discrepancies, it is tempting to attribute that the lack of superior efficacy of this agent at a higher dose to its poor solubility in aqueous solution. Thus, we recommend that future studies should consider the development and testing of water-soluble analogues or congeners of 6877002. Such studies are warranted and currently on-going in our laboratories.

RA is also characterised by systemic bone loss, and NFκB inhibition was found to alleviate bone destruction in RA models [44]. Surprisingly, we observed no differences in skeletal parameters between vehicle or 6877002 treated mice. This finding led us to tentatively conclude that 6877002 may not offer significant protection against systemic bone loss. Indeed, we failed to observe any significant effect by 6877002 on trabecular or cortical parameters of osteoporotic rats or RANKL-injected mice. Nevertheless, treatment of mice with 6877002 caused a modest – but non-significant – reduction in RANKL-induced bone loss. This finding is in agreement with the results of a pilot experiment in which 6877002 reduced ovariectomy-

induced bone loss in CD1 mice (conference abstract [45]). The discrepancies between these reports can only be attributed to species differences [46].

6877002 inhibits TRAF6/CD40 [26] and TRAF6/RANK signalling [27], two pathways that are implicated in the regulation of various downstream pathways, particularly NFκB and mitogen-activated protein (MAP) kinase pathways [10, 11, 42]. The MAP kinase pathway is implicated in RA [47, 48]. Although the precise mechanism(s) remains unclear, the evidence presented here shows that 6877002 inhibits RANKL-induced NFκB – but not ERK1/2 – activation, thereby leading us to speculate that MAP kinase activation may have contributed – at least in part – towards the inability of 6877002 to offer osteoprotective effect in the models of osteolysis described. Thus, we suggest that these paradoxical effects associated with TRAF6 inhibition should be carefully explored. For that, further studies are warranted and ongoing.

In recent decades, there have been concerted efforts to develop anti-inflammatory agents that selectively target and inhibit TRAF6/NFκB signalling for the treatment for diseases characterised by excessive joint and bone destruction. Very few agents have been tested or considered for approval by the authorities, we thus propose that TRAF6 inhibitors such as 6877002 or its future analogues/congeners can be of value in the management of the inflammatory component of conditions such as RA. However, these agents may not offer protection against systemic bone loss comparable to classic anti-resorptive therapy such as bisphosphonates. Furthermore, treatment of RA with classic anti-inflammatory agents such as dexamethasone or prednisolone often associated with drug-induced osteoporosis in patients [21, 22]. Thus, further studies are needed to test if and how 6877002 - or its novel analogues and congeners - exert anti-inflammatory and/or osteoprotection in other disease models.

5. CONFLICT OF INTERSET STATEMENT

A.I. Idris is a shareholder in a company (ArthElix Ltd., UK Registration No: 10597512) established to develop TRAF/NFκB inhibitors for the treatment of inflammatory disorders. P. Mollat, S. Meurisse and M. Auberval are employees of Galapagos SASU (102 Avenue Gaston Roussel, 93230 Romainville, France). G. Nicolaes and E. Lutgens are inventors in a patent to develop TRAF6/CD40 inhibitors for therapeutic use.

6. ETHICAL APPROVAL INFORMATION

Experimental protocols for studies described were approved by local Ethics Committees, as described under Materials and Methods.

7. PATIENT CONSENT FOR PUBLICATION

Not required.

8. CRediT AUTHORSHIP CONTRIBUTION STATEMENT

Silvia Marino: Investigation. Nicole Hannemann: Investigation, Formal analysis. Ryan T. Bishop: Investigation. Feier Zeng: Formal analysis. Giovana Carrasco: Investigation, Formal analysis. Sandrine Meurisse: Investigation. Boya Li: Formal analysis. Antonia Sophocleous: Formal analysis. Anna Sparatore: Conceptualization. Tobias Baeuerle: Investigation. Slobodan Vukicevic: Conceptualization, Supervision. Marielle Auberval: Investigation. Patrick Mollat: Conceptualization, Supervision. Aline Bozec: Conceptualization, Methodology, Supervision. Aymen I. Idris: Conceptualization, Supervision, Investigation, Methodology, Writing - Original Draft, Writing - Review & Editing.

9. FUNDING

This study did not receive specific grant from funding agencies in the public, commercial or not-for-profit sectors.

10. ACKNOWLEDGEMENTS

Special thanks to G. Nicolaes and E. Lutgens for donation of the patch of TRAF6/CD40 inhibitor 6877002 that was used in selected experiments.

ETHICAL APPROVAL INFORMATION

Experimental protocols for studies described were approved by local Ethics Committees.

REFERENCES

[1] D.L. Scott, F. Wolfe, T.W. Huizinga, Rheumatoid arthritis, Lancet 376(9746) (2010) 1094-108.

[2] Z. Chen, A. Bozec, A. Ramming, G. Schett, Anti-inflammatory and immune-regulatory cytokines in rheumatoid arthritis, Nat Rev Rheumatol 15(1) (2019) 9-17.

[3] J. Vilcek, M. Feldmann, Historical review: Cytokines as therapeutics and targets of therapeutics, Trends Pharmacol Sci 25(4) (2004) 201-9.

[4] M.H. Buch, S. Eyre, D. McGonagle, Persistent inflammatory and non-inflammatory mechanisms in refractory rheumatoid arthritis, Nat Rev Rheumatol 17(1) (2021) 17-33.

[5] F. Wolfe, The epidemiology of drug treatment failure in rheumatoid arthritis, Baillieres Clin Rheumatol 9(4) (1995) 619-32.

[6] B.G. Darnay, A. Besse, A.T. Poblenz, B. Lamothe, J.J. Jacoby, TRAFs in RANK signaling, Adv Exp Med Biol 597 (2007) 152-9.

[7] S.S. Pullen, M.E. Labadia, R.H. Ingraham, S.M. McWhirter, D.S. Everdeen, T. Alber, J.J. Crute, M.R. Kehry, High-affinity interactions of tumor necrosis factor receptor-associated factors (TRAFs) and CD40 require TRAF trimerization and CD40 multimerization, Biochemistry 38(31) (1999) 10168-10177.

[8] A.P. Armstrong, M.E. Tometsko, M. Glaccum, C.L. Sutherland, D. Cosman, W.C. Dougall, A RANK/TRAF6-dependent signal transduction pathway is essential for osteoclast cytoskeletal organization and resorptive function, J Biol.Chem. 277(46) (2002) 44347-44356.

[9] E. Jimi, I. Nakamura, T. Ikebe, S. Akiyama, N. Takahashi, T. Suda, Activation of NF-kappaB is involved in the survival of osteoclasts promoted by interleukin-1, Journal of Biological Chemistry 273(15) (1998) 8799-8805.

[10] C.C. Davies, T.W. Mak, L.S. Young, A.G. Eliopoulos, TRAF6 is required for TRAF2-dependent CD40 signal transduction in nonhemopoietic cells, Mol Cell Biol 25(22) (2005) 9806-19.

[11] M. Kashiwada, Y. Shirakata, J.I. Inoue, H. Nakano, K. Okazaki, K. Okumura, T. Yamamoto, H. Nagaoka, T. Takemori, Tumor necrosis factor receptor-associated factor 6 (TRAF6) stimulates extracellular signal-regulated kinase (ERK) activity in CD40 signaling along a ras-independent pathway, J Exp Med 187(2) (1998) 237-44.

[12] S. Kishida, H. Sanjo, S. Akira, K. Matsumoto, J. Ninomiya-Tsuji, TAK1-binding protein 2 facilitates ubiquitination of TRAF6 and assembly of TRAF6 with IKK in the IL-1 signaling pathway, Genes Cells 10(5) (2005) 447-454.

[13] J. Mizukami, G. Takaesu, H. Akatsuka, H. Sakurai, J. Ninomiya-Tsuji, K. Matsumoto, N. Sakurai, Receptor activator of NF-kappaB ligand (RANKL) activates TAK1 mitogen-activated protein kinase kinase kinase through a signaling complex containing RANK, TAB2, and TRAF6, Mol.Cell Biol. 22(4) (2002) 992-1000.

[14] B. Lamothe, W.K. Webster, A. Gopinathan, A. Besse, A.D. Campos, B.G. Darnay, TRAF6 ubiquitin ligase is essential for RANKL signaling and osteoclast differentiation, Biochem.Biophys.Res.Commun. 359(4) (2007) 1044-1049.

[15] X. Feng, RANKing intracellular signaling in osteoclasts, IUBMB.Life 57(6) (2005) 389-395.

[16] Y. Kadono, F. Okada, C. Perchonock, H.D. Jang, S.Y. Lee, N. Kim, Y. Choi, Strength of TRAF6 signalling determines osteoclastogenesis, EMBO Rep 6(2) (2005) 171-6.

[17] M.A. Lomaga, W.C. Yeh, I. Sarosi, G.S. Duncan, C. Furlonger, A. Ho, S. Morony, C. Capparelli, G. Van, S. Kaufman, H.A. van der, A. Itie, A. Wakeham, W. Khoo, T. Sasaki, Z. Cao, J.M. Penninger, C.J. Paige, D.L. Lacey, C.R. Dunstan, W.J. Boyle, D.V. Goeddel, T.W. Mak, TRAF6 deficiency results in osteopetrosis and defective interleukin-1, CD40, and LPS signaling, Genes Dev. 13(8) (1999) 1015-1024.

[18] N. Kobayashi, Y. Kadono, A. Naito, K. Matsumoto, T. Yamamoto, S. Tanaka, J. Inoue, Segregation of TRAF6-mediated signaling pathways clarifies its role in osteoclastogenesis, EMBO Journal 20(6) (2001) 1271-1280.

[19] A. Naito, S. Azuma, S. Tanaka, T. Miyazaki, S. Takaki, K. Takatsu, K. Nakao, K. Nakamura, M. Katsuki, T. Yamamoto, J. Inoue, Severe osteopetrosis, defective interleukin-1 signalling and lymph node organogenesis in TRAF6-deficient mice, Genes Cells 4(6) (1999) 353-362.
[20] B. Osta, G. Benedetti, P. Miossec, Classical and Paradoxical Effects of TNF-alpha on Bone Homeostasis, Front Immunol 5 (2014) 48.
[21] L.M. Sedger, M.F. McDermott, TNF and TNF-receptors: From mediators of cell death and inflammation to therapeutic giants – past, present and future, Cytokine & Growth Factor Reviews 25(4) (2014) 453-472.
[22] C. Monaco, J. Nanchahal, P. Taylor, M. Feldmann, Anti-TNF therapy: past, present and future, Int Immunol 27(1) (2015) 55-62.
[23] M. Funakoshi-Tago, N. Kamada, T. Shimizu, Y. Hashiguchi, K. Tago, Y. Sonoda, T. Kasahara, TRAF6 negatively regulates TNFalpha-induced NF-kappaB activation, Cytokine 45(2) (2009) 72-9.
[24] R. Tewari, S.R. Choudhury, V.S. Mehta, E. Sen, TNFalpha regulates the localization of CD40 in lipid rafts of glioma cells, Mol Biol Rep 39(9) (2012) 8695-9.
[25] Y.H. Zhang, A. Heulsmann, M.M. Tondravi, A. Mukherjee, Y. Abu-Amer, Tumor necrosis factor-alpha (TNF) stimulates RANKL-induced osteoclastogenesis via coupling of TNF type 1 receptor and RANK signaling pathways, J.Biol.Chem. 276(1) (2001) 563-568.
[26] B. Zarzycka, T. Seijkens, S.B. Nabuurs, T. Ritschel, J. Grommes, O. Soehnlein, R. Schrijver, C.M. van Tiel, T.M. Hackeng, C. Weber, F. Giehler, A. Kieser, E. Lutgens, G. Vriend, G.A. Nicolaes, Discovery of small molecule CD40-TRAF6 inhibitors, J Chem Inf Model 55(2) (2015) 294-307.
[27] R.T. Bishop, S. Marino, G. Carrasco, B. Li, R.J. Allen, A. Sparatore, P.D. Ottewell, P. Mollat, A.H. Sims, M. Capulli, N. Wang, A.I. Idris, Combined administration of a small-molecule inhibitor of TRAF6 and Docetaxel reduces breast cancer skeletal metastasis and osteolysis, Cancer Lett 488 (2020) 27-39.
[28] N. Kim, Y. Kadono, M. Takami, J. Lee, S.H. Lee, F. Okada, J.H. Kim, T. Kobayashi, P.R. Odgren, H. Nakano, W.C. Yeh, S.K. Lee, J.A. Lorenzo, Y. Choi,

Osteoclast differentiation independent of the TRANCE-RANK-TRAF6 axis, J Exp Med 202(5) (2005) 589-95.
[29] T.T. Seijkens, C.M. van Tiel, P.J. Kusters, D. Atzler, O. Soehnlein, B. Zarzycka, S.A. Aarts, M. Lameijer, M.J. Gijbels, L. Beckers, M. den Toom, B. Slütter, J. Kuiper, J. Duchene, M. Aslani, R.T. Megens, C. van 't Veer, G. Kooij, R. Schrijver, M.A. Hoeksema, L. Boon, F. Fay, J. Tang, S. Baxter, A. Jongejan, P.D. Moerland, G. Vriend, B. Bleijlevens, E.A. Fisher, R. Duivenvoorden, N. Gerdes, M.P. de Winther, G.A. Nicolaes, W.J. Mulder, C. Weber, E. Lutgens, Targeting CD40-Induced TRAF6 Signaling in Macrophages Reduces Atherosclerosis, J Am Coll Cardiol 71(5) (2018) 527-42.
[30] B. Grotsch, A. Bozec, G. Schett, In Vivo Models of Rheumatoid Arthritis, Methods Mol Biol 1914 (2019) 269-280.
[31] R.J. van 't Hof, E. Dall'Ara, Analysis of Bone Architecture in Rodents Using Micro-Computed Tomography, Methods Mol Biol 1914 (2019) 507-531.
[32] A. Sophocleous, A.I. Idris, Ovariectomy/Orchiectomy in Rodents, Methods Mol Biol 1914 (2019) 261-267.
[33] S. Marino, R.T. Bishop, D. de Ridder, J. Delgado-Calle, M.R. Reagan, 2D and 3D In Vitro Co-Culture for Cancer and Bone Cell Interaction Studies, Methods Mol Biol 1914 (2019) 71-98.
[34] N. Rucci, A. Zallone, A. Teti, Isolation and Generation of Osteoclasts, Methods Mol Biol 1914 (2019) 3-19.
[35] I.P. Perpetuo, L.E. Bourne, I.R. Orriss, Isolation and Generation of Osteoblasts, Methods Mol Biol 1914 (2019) 21-38.
[36] G.R. Nakayama, M.C. Caton, M.P. Nova, Z. Parandoosh, Assessment of the Alamar Blue assay for cellular growth and viability in vitro, J.Immunol.Methods 204(2) (1997) 205-208.
[37] S. Marino, A.I. Idris, Analysis of Signaling Pathways by Western Blotting and Immunoprecipitation, Methods Mol Biol 1914 (2019) 131-143.
[38] E.M. Gravallese, D.L. Galson, S.R. Goldring, P.E. Auron, The role of TNF-receptor family members and other TRAF-dependent receptors in bone resorption, Arthritis Res 3(1) (2001) 6-12.

[39] L. D'Amico, I. Roato, Cross-talk between T cells and osteoclasts in bone resorption, Bonekey Rep 1 (2012) 82.
[40] J.Y. Li, H. Tawfeek, B. Bedi, X. Yang, J. Adams, K.Y. Gao, M. Zayzafoon, M.N. Weitzmann, R. Pacifici, Ovariectomy disregulates osteoblast and osteoclast formation through the T-cell receptor CD40 ligand, Proc Natl Acad Sci U S A 108(2) (2011) 768-73.
[41] J.Y. Li, J. Adams, L.M. Calvi, T.F. Lane, M.N. Weitzmann, R. Pacifici, Ovariectomy expands murine short-term hemopoietic stem cell function through T cell expressed CD40L and Wnt10B, Blood 122(14) (2013) 2346-57.
[42] A.G. Eliopoulos, C.C. Wang, C.D. Dumitru, P.N. Tsichlis, Tpl2 transduces CD40 and TNF signals that activate ERK and regulates IgE induction by CD40, EMBO J 22(15) (2003) 3855-64.
[43] D.P. O'Doherty, B.J. Gertz, W. Tindale, D.G. Sciberras, T.T. Survill, J.A. Kanis, Effects of five daily 1 h infusions of alendronate in Paget's disease of bone, Journal of Bone and Mineral Research 7 (1992) 81-87.
[44] Y. Okazaki, T. Sawada, K. Nagatani, Y. Komagata, T. Inoue, S. Muto, A. Itai, K. Yamamoto, Effect of nuclear factor-kappaB inhibition on rheumatoid fibroblast-like synoviocytes and collagen induced arthritis, J Rheumatol 32(8) (2005) 1440-7.
[45] S.B. Marino, R.; Bendle, G.; Nicolaes, G.; Lutgens, E.; Idris, A.I, A small molecule inhibitor of TRAF6 dependent signaling reduces osteoclastogenesis and prevents ovariectomy induced bone loss, Bone 1 (2016) S.
[46] A.S. Turner, Animal models of osteoporosis--necessity and limitations, Eur Cell Mater 1 (2001) 66-81.
[47] G. Schett, J. Zwerina, G. Firestein, The p38 mitogen-activated protein kinase (MAPK) pathway in rheumatoid arthritis, Ann Rheum Dis 67(7) (2008) 909-16.
[48] D. de Launay, M.G. van de Sande, M.J. de Hair, A.M. Grabiec, G.P. van de Sande, K.A. Lehmann, C.A. Wijbrandts, L.G. van Baarsen, D.M. Gerlag, P.P. Tak, K.A. Reedquist, Selective involvement of ERK and JNK mitogen-activated protein kinases in early rheumatoid arthritis (1987 ACR criteria compared to 2010 ACR/EULAR criteria): a prospective study aimed at identification of diagnostic and prognostic biomarkers as well as therapeutic targets, Ann Rheum Dis 71(3) (2012) 415-23.

Figure legends

Fig. 1. 6877002 reduces TNFα-induced NFκB activation, osteoclastogenesis and osteolysis. (***a***) The chemical structure of the small-molecule inhibitor of TRAF6 6877002. (***b***) Graphic representation of *ex vivo* mouse calvarial organ system pretreated with vehicle or 6877002 (10 μM) in the presence or absence of TNFα (20 ng/ml) for 5 days. (***c***) *ex vivo* bone volume (BV) and osteolysis in the mouse calvarial organ co-culture system described in panel ***b***. Schematic was created with BioRender.com under a paid subscription. (***d***) *In vitro* osteoclast formation in RANKL (50 – 200 ng/ml) stimulated human pre-osteoclasts treated with vehicle or 6877002 (up to 3 μM) for 72 hours in the presence and absence of TNFα (10 ng/ml), as assessed by TRAcP staining assay. (***e***) Representative photomicrographs of TRAcP positive mature human osteoclasts from the experiment described in panel ***c*** (scale bar = 50 μm). (***f***) *In vitro* viability of M-CSF generated human pre-osteoclasts treated with vehicle or 6877002 (0 – 3.0 μM), as assessed by AlamarBlue assay. (***g***) *In vitro* NFκB activation assessed by western blot quantification of phosphorylated (left) and total (right) IκBα in mouse pre-osteoclast-like RAW 264.7 macrophages pre-treated with vehicle or 6877002 (0 – 50 μM) for 1 hour prior exposure to TNFα (10 ng/ml) for 10 minutes. (***h***) Representative photomicrographs of blots from the experiment described in panel ***g***. (***i***) *In vitro* quantification of osteoclast number in calvarial osteoblast – bone marrow cells co-cultures pre-treated with vehicle or 6877002 (up to 3 μM) for 72 hours in the presence and absence of TNFα (20 ng/ml), as assessed by TRAcP staining assay. (***j***) *In vitro* osteoblast viability in cultures of primary mouse calvarial pre-osteoblasts treated with vehicle or 6877002 (0 – 10 μM) in the presence and absence of TNFα (20 and 100 ng/ml) for 5 days, as assessed by AlamarBlue

assay. (***k***) *In vitro* caspase-3/7 activation in primary calvarial pre-osteoblasts from the experiment described in panel ***j***. (***l***) *In vitro* osteoblast viability (left) and bone nodule formation (right) in cultures of human Saos2 and mouse MC3T3 pre-osteoblasts treated with vehicle or 6877002 (0 – 3.0 μM) for 21 days, as assessed by AlamarBlue and Alazarin Red (ALZ) assays, respectively. Values are mean ± SD of three independent experiments (n = 3) unless stated otherwise; * $p<0.05$ and ** $p<0.01$ from vehicle; # $p < 0.05$ from control plus TNFα; + $p < 0.05$ from control plus RANKL (50 ng/ml); $ $p < 0.05$ from control plus RANKL (100 ng/ml); XX $p < 0.05$ from vehicle plus TNFα. Dotted line denotes control. Abbreviation: M, molecular weight marker; kD, kilodalton.

Fig. 2. 6877002 disrupts T Lymphocytes crosstalk with osteoclasts and synoviocytes, but not osteoblasts. (***a***) *In vitro* chemotactic 2D migration of human synoviocyte-like SW982 cells treated with vehicle or 6877002 (0 – 3.0 μM) in the presence of conditioned medium (CM, 20%, v/v) from naïve or active Jurkat E6.1 T Lymphocytes for 16 hours, as assessed by wound healing assay. Representative photomicrographs show cultures of human SW982 synoviocytes from the experiment described (panel ***a***, right) (scale bar = 50 μm). (***b***) *In vitro* osteoclast formation in RANKL (100 ng/ml) stimulated human pre-osteoclasts treated with vehicle or 6877002 (3 μM) in the presence of active Jurkat E6.1 T Lymphocytes CM (20%, v/v) for 72 hours, as assessed by TRAcP staining assay. Representative photomicrographs show TRAcP positive mature human osteoclasts from the experiment described (panel ***b***, right) (scale bar = 50 μm). (***c***) *In vitro* viability of human pre-osteoclasts pretreated with vehicle or 6877002 (0 – 3.0 μM) in the presence of conditioned medium (CM, 20%, v/v) from activated human T-cell-like Jurkat E6.1 cells for 72 hours, as assessed by AlamarBlue assay. (***d***) *In vitro* osteoblast viability in cultures

of mouse MC3T3 pre-osteoblasts treated with vehicle or 6877002 (0 - 3.0 μM) in the presence of active Jurkat E6.1 T Lymphocytes CM (20%, v/v) for 72 hours, as assessed by AlamarBlue assay. Values are mean ± SD of three independent experiments (n = 3) unless stated otherwise; * $p<0.05$ and ** $p<0.01$ from vehicle; + + $p < 0.01$ from control plus naïve Jurkat E6.1 cell CM (20%, v/v).

Fig. 3. Oral and intraperitoneal administration of 6877002 reduces clinical arthritis score in mice. (***a-b***) Graphic representation (left) and experiment timeline (right) of intraperitoneal (IP, 20 mg/kg/thrice-weekly, **a**) or oral (gavage, 50 mg/kg/thrice-weekly, **b**) administration of vehicle or 6877002 into 6-week old DBA/1 mice subjected to CIA (n = 10/group). Schematic was created with BioRender.com under a paid subscription. (***c***) Combined area under the curve (AUC) from IP and oral experiments descried in panels ***a*** *and* ***b***. (***d - e***) hind paw thickness (***d***) and arthritic score in hind paws and ankles (***e***) in mice from the experiment described in panel **a**. (***f - g***) Quantification of soft tissue (***f***) and bone marrow volume (***g***) from T1 and T2 relaxation time in mice from IP and oral experiments descried in panels ***a*** *and* ***d***. (***h - i***) Representative photomicrographs of MRI scans of mouse paws from the experiments described in panels ***a*** – ***g*** (scale bar = 5 mm). Arrows indicate synovial thickening. Values are mean ± SEM; * $p<0.05$ and ** $p<0.01$ from vehicle treated group. AUC denotes area under the curve; ms, milli-second(s).

Fig. 4. Oral and intraperitoneal administration of 6877002 has no effect on bone loss in arthritic mice. (***a - d***) *In vivo* trabecular bone volume (Tb.BV/TV, ***a***), number (Tb.N., ***b***), thickness (Tb.Th., ***c***), trabecular separation (Tb.Sp., ***d***) at the tibia of arthritic mice subjected to CIA and intraperitoneal (IP) or oral (gavage) treatment of vehicle or 6877002 (IP: 20 and Oral: 50 mg/kg/thrice-weekly) for 45 days (IP: n = 16/group and

Oral: n = 14/group), as assessed by microCT. (***e***) Representative photomicrographs of microCT scans of mouse trabecular compartment from the experiment (scale bar = 1 mm). (***f*** **-** ***g***) *In vivo* cortical bone (Ct.) volume (Ct.BV/TV, ***f***) and thickness (Ct.Th., ***g***) at the tibia of arthritic mice from the experiment described in panels ***a*** **-** ***e***, as assessed by microCT. (***h***) Representative photomicrographs of microCT scans of mouse cortical and trabecular compartments from the experiment (scale bar = 1 mm). Values are mean ± SD.

Fig. 5. 6877002 has no effect on bone loss in oestrogen-deficient osteoporotic rats. (***a***) Graphic representation of intraperitoneal (IP) administration of vehicle or 6877002 (20 mg/kg/thrice-weekly) in female Sprague Dawley rats (4-5 month old) subjected to ovariectomy (ovx) for 3 weeks (n = 9/group). (***b***) *In vivo* trabecular bone volume (Tb.BV/TV) at the tibia (left), femur (middle), spine (right) from the experiment described in panel ***a***, as assessed by microCT. Schematic was created with BioRender.com under a paid subscription. (***d***) *In vivo* cortical bone volume (Ct.BV/TV) at the tibia (left) and femur (right) from the experiment described in panels ***a*** and ***b***. (***d*** - ***f***) Representative photomicrographs of microCT scans of the tibia (***d***), femur (***e***) and spine (***f***) of mice from the experiment described in panels ***a*** – ***g*** (scale bar = 1 mm). Values are mean ± SD. * $p<0.05$; ** $p<0.01$ from sham control.

Fig. 6. 6877002 has no effect on RANKL-induced MAPK activation *in vitro* or osteoporosis in mice. (***a***) *In vitro* NFκB and MAPK activation assessed by western blot quantification of phosphorylated (phospho-) IκBα, ERK42, ERK44, P38 and JNK1/2 in mouse M-CSF generated pre-osteoclasts pretreated with vehicle or 6877002 (0 - 30μM) for 1 hour and exposed to soluble sRANKL (200 ng/ml) for 15 minutes. Values are mean ± SD of three independent experiments (n = 3). Dotted line denotes control. (***b*** **-** ***c***)

Graphic representation (***b***) and experiment timeline (***c***) of administration of vehicle or 6877002 (IP, 10 or 20 mg/kg/day 1 to 4) or Alendronate (ALN, SC, 60 mg/kg/day -3, 0 and 2) in 8-week-old female C3H mice injected daily with sRANKL (1 mg/kg) for 4 days (n = 10 mice/group). Schematic was created with BioRender.com under a paid subscription. (***d - e***) *In vivo* trabecular bone volume (Tb.BV/TV) at the tibia of the osteotropic mice described, as assessed by microCT. Representative photomicrographs of microCT scans of the tibia of mice from the experiment are shown in panel e (scale bar = 1 mm). (***f - h***) *in vivo* trabecular number (Tb.N., ***f***), thickness (Tb.Th., ***g***), trabecular separation (Tb.Sp., ***h***) at the tibia the osteotropic mice described in panels a-e.; Values are mean ± SD (n = 10). ** $p<0.01$ from vehicle and ++ $p < 0.01$ from control plus sRANKL.

Figures

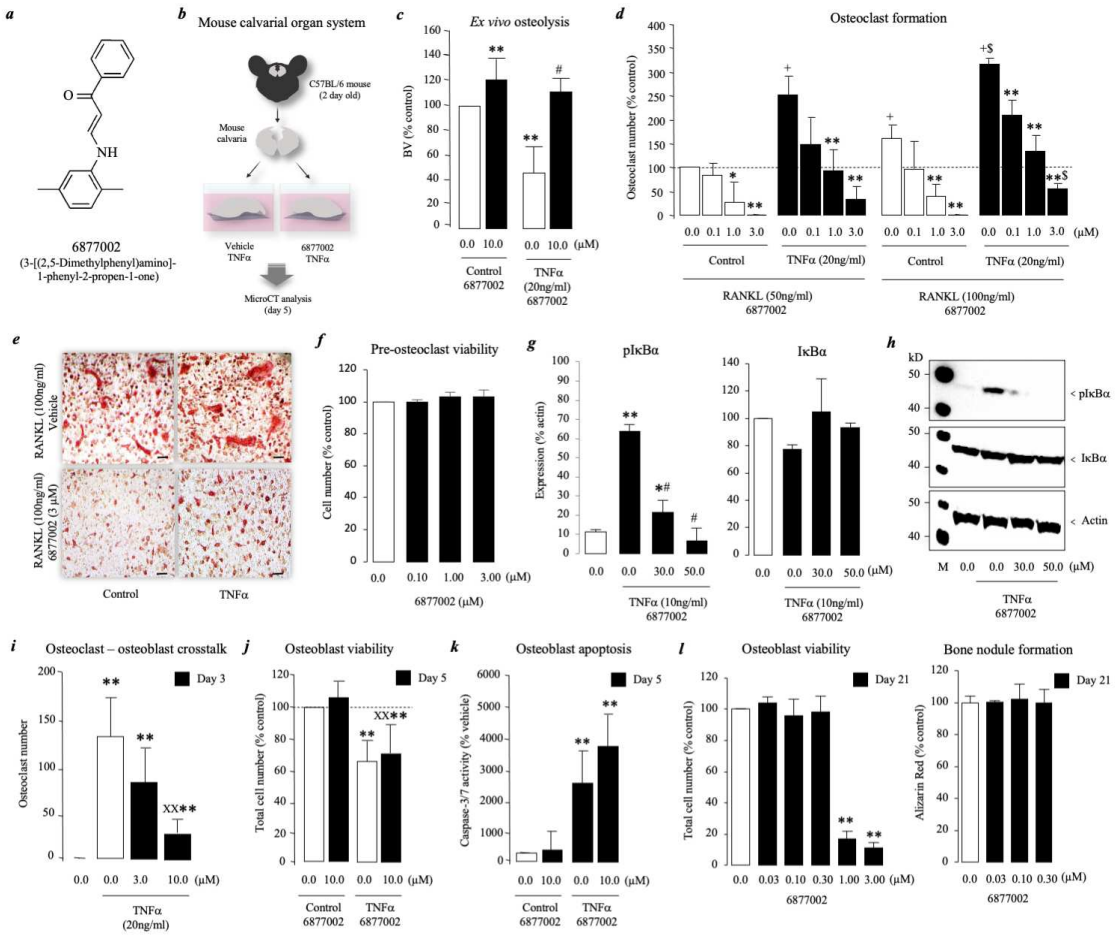
a
6877002
(3-[(2,5-Dimethylphenyl)amino]-
1-phenyl-2-propen-1-one)
b
Mouse calvarial organ system
C57BL/6 mouse
(2 day old)
Mouse
calvaria
Vehicle
TNFα
6877002
TNFα
MicroCT analysis
(day 5)
c
Ex vivo osteolysis
BV (% control)
Control
6877002
TNFα
(20ng/ml)
6877002
d
Osteoclast formation
Osteoclast number (% control)
Control
TNFα (20ng/ml)
RANKL (50ng/ml)
6877002
RANKL (100ng/ml)
6877002
e
RANKL (100ng/ml)
Vehicle
RANKL (100ng/ml)
6877002 (3 μM)
Control
TNFα
f
Pre-osteoclast viability
Cell number (% control)
6877002 (μM)
g
pIκBα
IκBα
Expression (% actin)
TNFα (10ng/ml)
6877002
h
kD
< pIκBα
< IκBα
< Actin
M
TNFα
6877002
i
Osteoclast – osteoblast crosstalk
Day 3
Osteoclast number
TNFα
(20ng/ml)
j
Osteoblast viability
Day 5
Total cell number (% control)
Control
6877002
TNFα
6877002
k
Osteoblast apoptosis
Day 5
Caspase-3/7 activity (% vehicle)
Control
6877002
TNFα
6877002
l
Osteoblast viability
Day 21
Total cell number (% control)
6877002
Bone nodule formation
Day 21
Alizarin Red (% control)
6877002

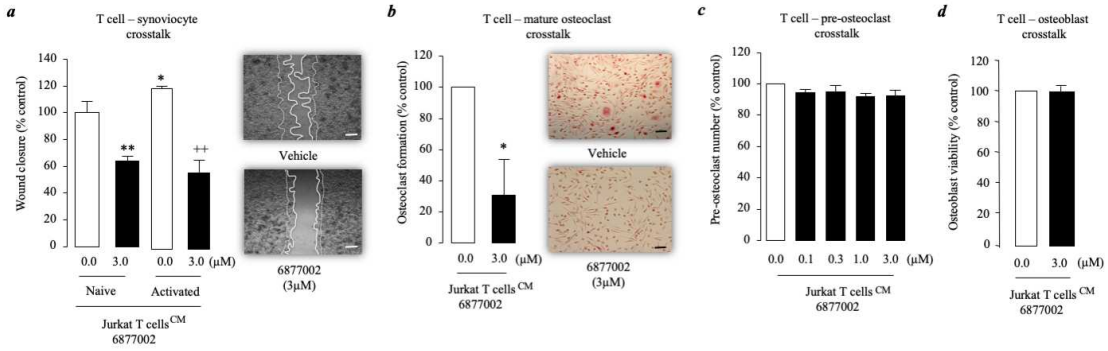
a
T cell – synoviocyte crosstalk
Wound closure (% control)
140
120
100
80
60
40
20
0
**
*
++
0.0
3.0
0.0
3.0 (μM)
Naive
Activated
Jurkat T cells CM 6877002
Vehicle
6877002 (3μM)
b
T cell – mature osteoclast crosstalk
Osteoclast formation (% control)
120
100
80
60
40
20
0
*
0.0
3.0 (μM)
Jurkat T cells CM 6877002
Vehicle
6877002 (3μM)
c
T cell – pre-osteoclast crosstalk
Pre-osteoclast number (% control)
120
100
80
60
40
20
0
0.0
0.1
0.3
1.0
3.0 (μM)
Jurkat T cells CM 6877002
d
T cell – osteoblast crosstalk
Osteoblast viability (% control)
120
100
80
60
40
20
0
0.0
3.0 (μM)
Jurkat T cells CM 6877002

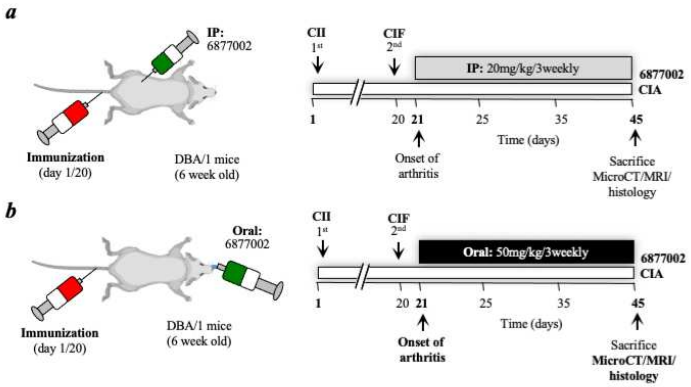

c

Paw thickness
(area under the curve, AUC)

	Drug	AUC
IP	vehicle	18.56 ± 3.1
	6877002	8.44 ± 2.1**
Oral	vehicle	53.60 ± 1.1
	6877002	51.07 ± 0.64*

** $p < 0.01$ and * $p < 0.05$ versus respective vehicle.

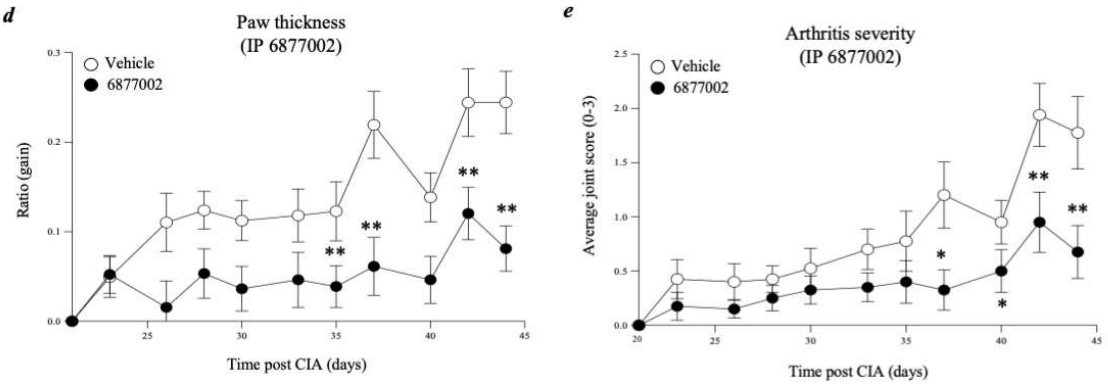

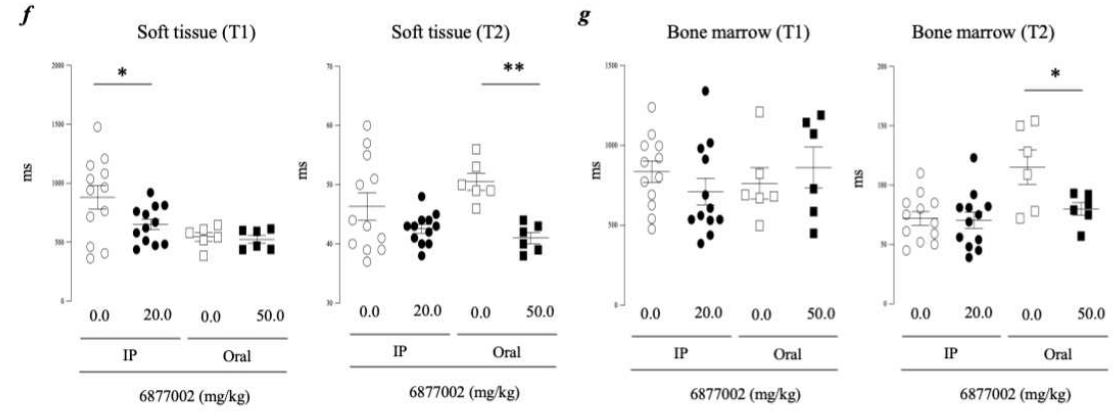

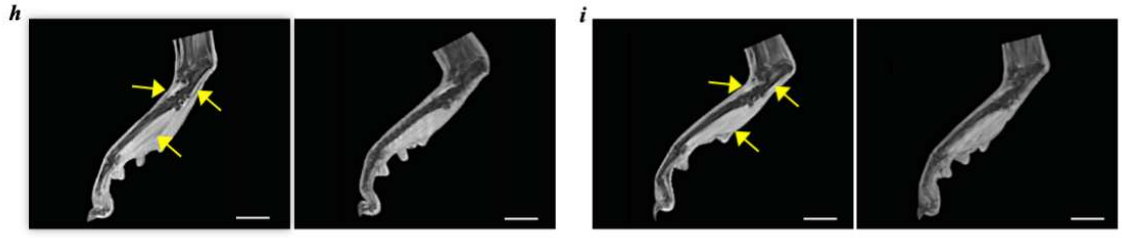

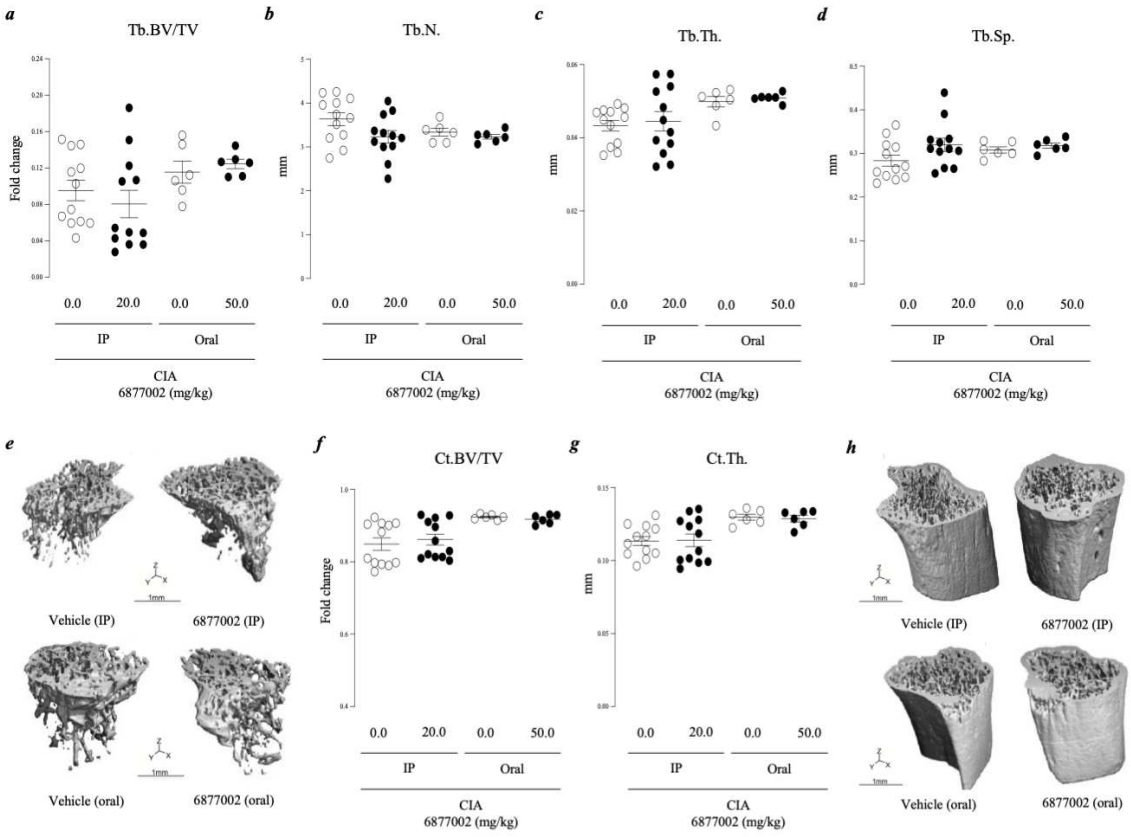
a
Tb.BV/TV
Fold change
b
Tb.N.
mm
c
Tb.Th.
mm
d
Tb.Sp.
mm
0.0
20.0
0.0
50.0
IP
Oral
CIA
6877002 (mg/kg)
e
Vehicle (IP)
6877002 (IP)
Vehicle (oral)
6877002 (oral)
1mm
f
Ct.BV/TV
Fold change
g
Ct.Th.
mm
h
Vehicle (IP)
6877002 (IP)
Vehicle (oral)
6877002 (oral)

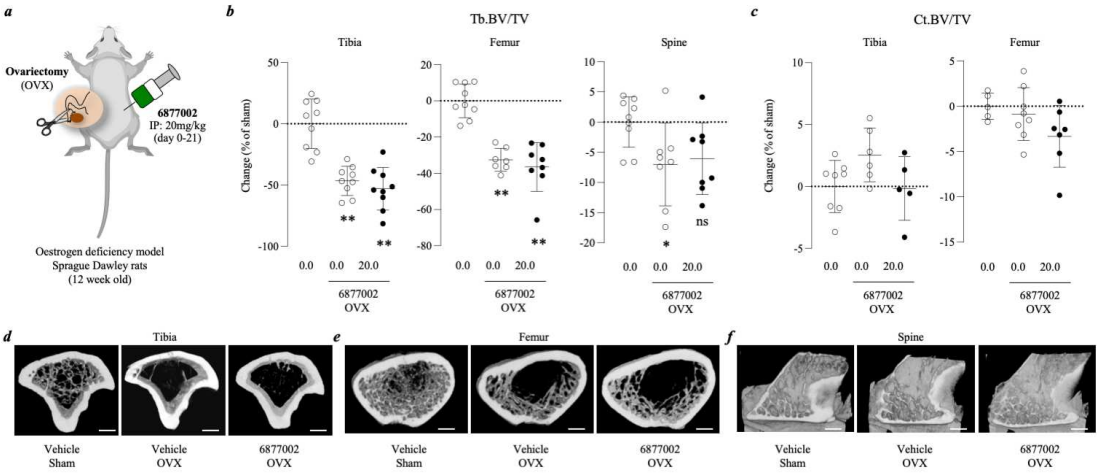
a
Ovariectomy
(OVX)
6877002
IP: 20mg/kg
(day 0-21)
Oestrogen deficiency model
Sprague Dawley rats
(12 week old)
b
Tb.BV/TV
Tibia
Femur
Spine
Change (% of sham)
0.0
0.0
20.0
6877002
OVX
ns
c
Ct.BV/TV
Tibia
Femur
d
Tibia
e
Femur
f
Spine
Vehicle
Sham
Vehicle
OVX
6877002
OVX

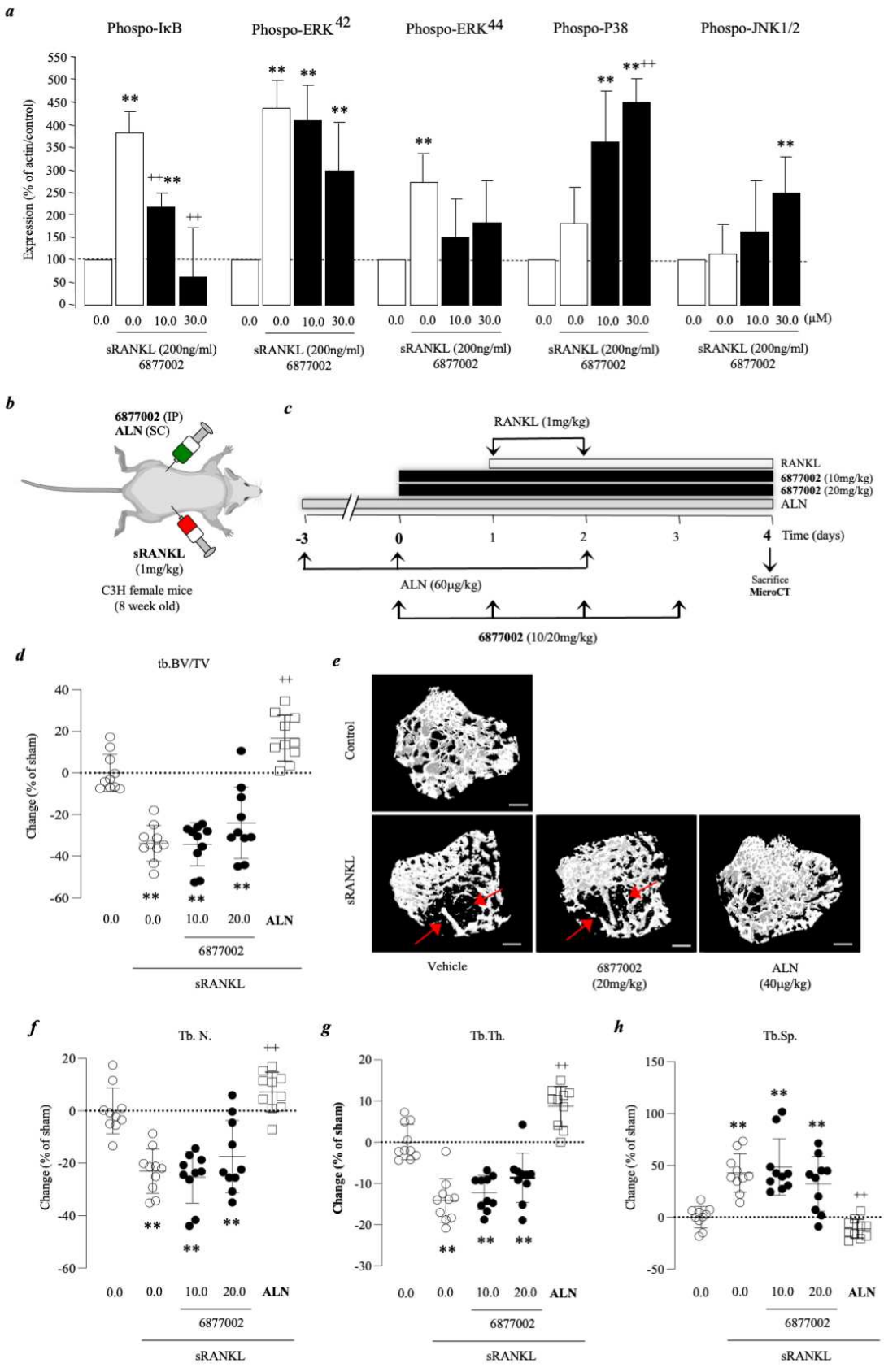
a
Phospo-IκB
Phospo-ERK42
Phospo-ERK44
Phospo-P38
Phospo-JNK1/2
Expression (% of actin/control)
sRANKL (200ng/ml)
6877002
(μM)
b
6877002 (IP)
ALN (SC)
sRANKL
(1mg/kg)
C3H female mice
(8 week old)
c
RANKL (1mg/kg)
RANKL
6877002 (10mg/kg)
6877002 (20mg/kg)
ALN
Time (days)
Sacrifice
MicroCT
ALN (60μg/kg)
6877002 (10/20mg/kg)
d
tb.BV/TV
Change (% of sham)
ALN
6877002
sRANKL
e
Control
sRANKL
Vehicle
6877002
(20mg/kg)
ALN
(40μg/kg)
f
Tb. N.
g
Tb.Th.
h
Tb.Sp.

SUPPLEMTARY FIGURES

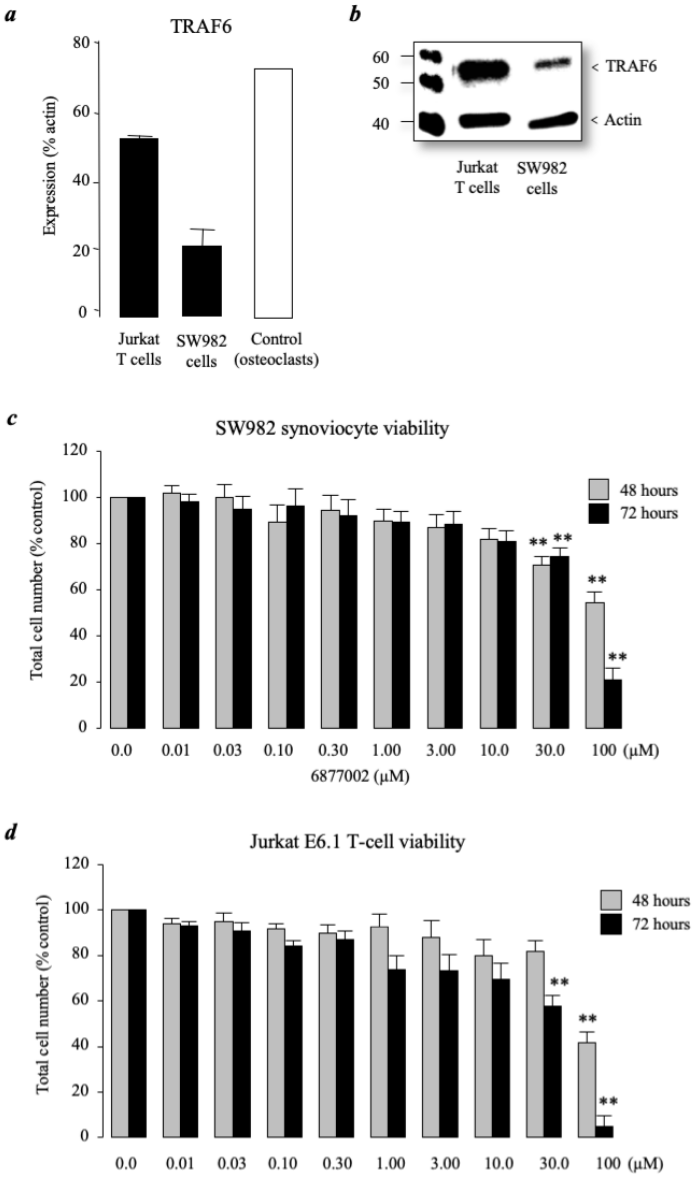

Supplementary Figure S1 (related to Figure 1 and 2). (***a*** **-** ***b***) TRAF6 expression in human Jurkat E6.1 T Lymphocytes, synoviocyte-like SW982 cells and osteoclasts (n = 1), as assessed by western blot analysis. Effects of 6877002 (0-100µM) on *in vitro* viability in cultures of Jurkat E6.1 T-cells (***d***) and SW982 cells (***c***) for 48 and 72 hours, as assessed by AlamarBlue. Values are mean ± SD of three independent experiments (n = 3) unless stated otherwise; ** $p<0.01$ from vehicle.

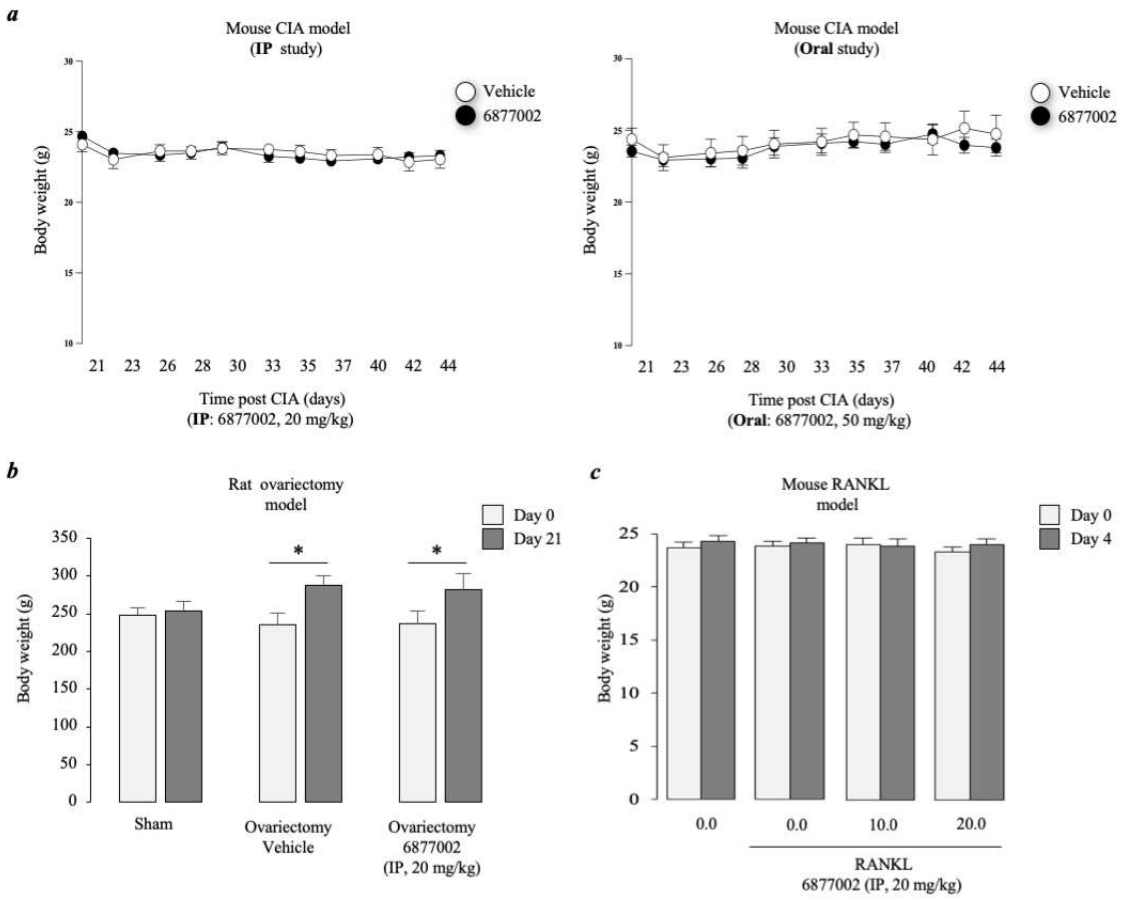

Supplementary Figure S2 (related to Figures 3 to 6). Body weight in arthritic mice (***a***, related to Fig. 3 and 4), ovariectomized (ovx) rats (***b***, related to Fig. 5) and mice subjected to RANKL treatment (***c***, related to Fig. 6). Values are mean ± SD. * $p<0.05$.

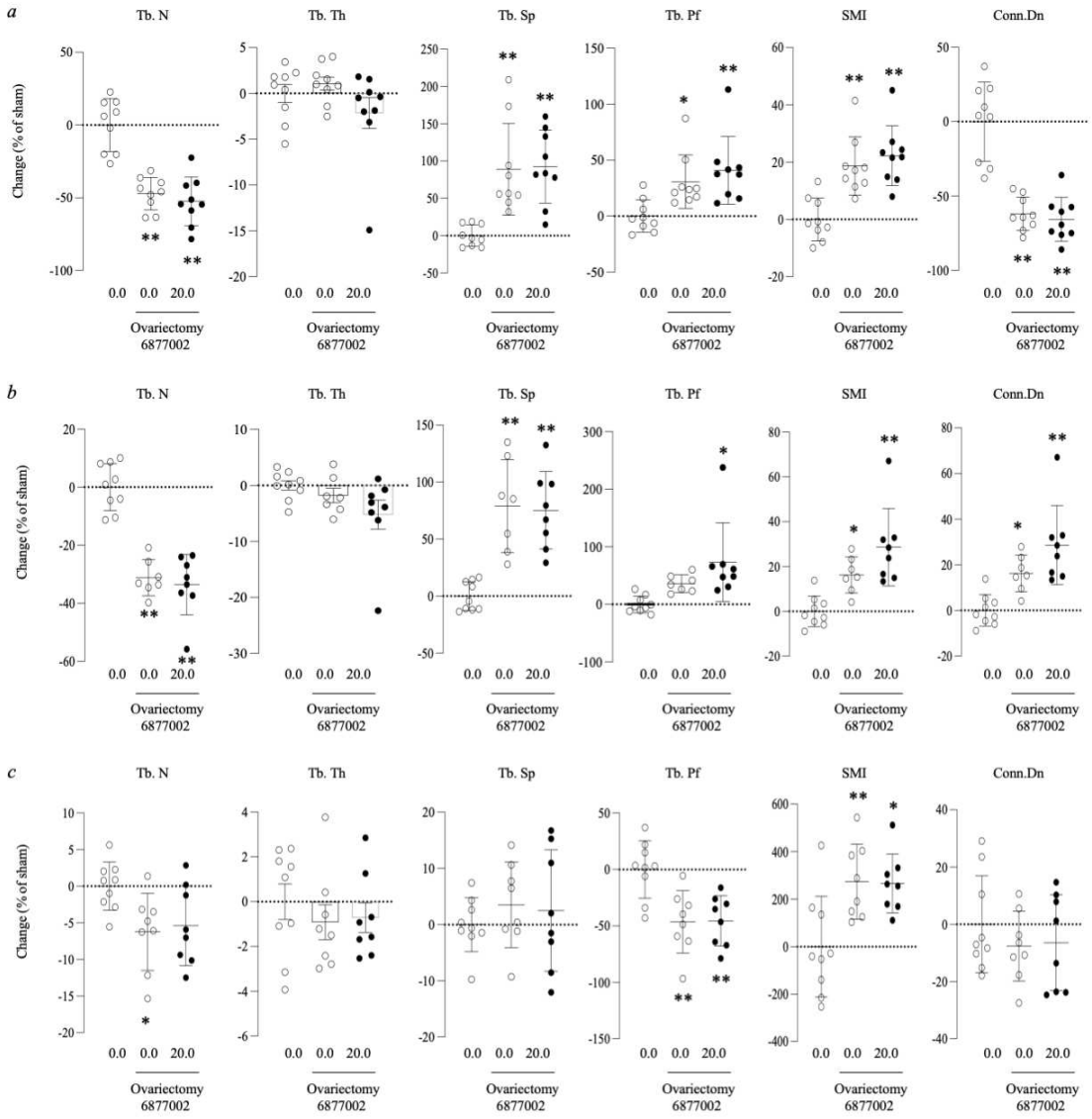

Supplementary Figure S3 (related to Figure 5). Effect of 6877002 on bone loss in oestrogen-deficient osteoporotic rats. *in vivo* trabecular number (Tb.) number (Tb.N.), thickness (Tb.Th.), separation, (Tb.Sp.), pattern factor (Tb.Pf.), SMI and connectivity density (Conn.Dn.) at the tibia (***a***), femur (***b***) and spine (***c***) from the experiment described in Figures 5. Values are mean ± SD. * $p<0.05$; ** $p<0.01$ from sham control.

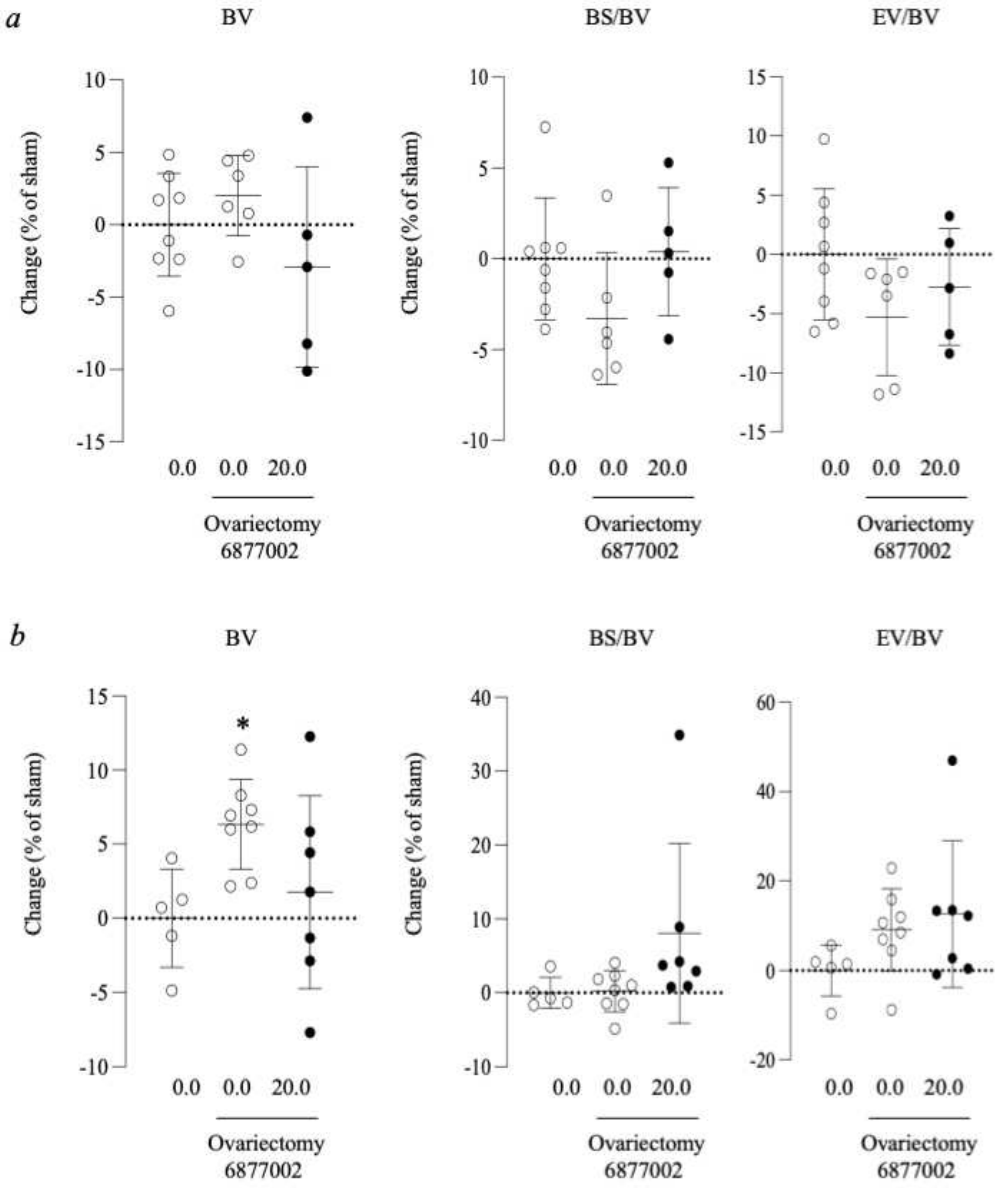

Figure S4 (related to Figure 5). Effect of 6877002 on bone loss in oestrogen-deficient osteoporotic rats. *In vivo* changes in cortical (Ct.) bone (BV, mm^3), bone surface (BS/TV) and endocortical surface (EV/BV) volumes at the tibia (***a***) and femur (***b***) from the experiment described in Figures 5. Values are mean ± SD. * $p < 0.05$.